

# Second-order accurate ensemble transform particle filters

Jana de Wiljes\*

Walter Acevedo<sup>†</sup>

Sebastian Reich<sup>‡</sup>

October 19, 2022

## Abstract

Particle filters (also called sequential Monte Carlo methods) are widely used for state and parameter estimation problems in the context of nonlinear evolution equations. The recently proposed ensemble transform particle filter (ETPF) (S. Reich, *A non-parametric ensemble transform method for Bayesian inference*, SIAM J. Sci. Comput., 35, (2013), pp. A2013–A2014) replaces the resampling step of a standard particle filter by a linear transformation which allows for a hybridization of particle filters with ensemble Kalman filters and renders the resulting hybrid filters applicable to spatially extended systems. However, the linear transformation step is computationally expensive and leads to an underestimation of the ensemble spread for small and moderate ensemble sizes. Here we address both of these shortcomings by developing second-order accurate extensions of the ETPF. These extensions allow one in particular to replace the exact solution of a linear transport problem by its Sinkhorn approximation. We demonstrate the performance of the second-order accurate filters for a single non-Gaussian data assimilation step, the chaotic Lorenz-63 model, and a scene-viewing model.

**Keywords.** Bayesian inference, data assimilation, particle filter, ensemble Kalman filter, Sinkhorn approximation

**AMS(MOS) subject classifications.** 65C05, 62M20, 93E11, 62F15, 86A22

## 1 Introduction

Data assimilation (DA) denotes the broad topic of combining evolution models with partial observations of the underlying dynamical process [8, 11, 17]. DA algorithms come in the form of variational and/or ensemble-based methods [11]. In this paper, we focus on ensemble-based DA methods and their robust and efficient implementation. The ensemble Kalman filter (EnKF) [8] is by far the most popular ensemble-based DA method and has found widespread application in the geosciences. However, EnKFs lead to inconsistent approximations for partially observed nonlinear processes. On the contrary, particle filters (PF) (also called sequential Monte Carlo methods) [6] lead to consistent approximations but typically require ensemble sizes much larger than those required for EnKFs in order to track the underlying reference process [2].

In order to overcome these shortcomings, we are currently witnessing a strong trend towards hybrid filters which combine EnKFs with PFs and which are applicable to strongly nonlinear systems under small or moderate ensemble sizes. We mention here the Gaussian mixture filters (such as, for example, [19]), the rank histogram filter [1, 14], moment matching ensemble filters [23, 12, 20], the ensemble Kalman particle filter [9], and the hybrid ensemble transform particle filter [4].

In this paper, we focus on improved implementations of the ensemble transform particle filter (ETPF) [16, 17] and its hybridization with the EnKF [4]. The ETPF requires the solution of a linear transport problem in each assimilation step, which renders the methods substantially more expensive than an EnKF. Computationally attractive alternatives, such as the Sinkhorn approximation [5], lead to unstable implementations since the ensemble becomes underdispersive. We address this problem by introducing a variant of the ETPF, which is second-order accurate independent of the actual solution procedure for the underlying optimal transport problem. An ensemble filter is called second-order accurate if the posterior mean and covariance matrix of the

\*Universität Potsdam, Institut für Mathematik, Karl-Liebknecht-Str. 24/25, D-14476 Potsdam, Germany

<sup>†</sup>Universität Potsdam, Institut für Mathematik, Karl-Liebknecht-Str. 24/25, D-14476 Potsdam, Germany

<sup>‡</sup>Universität Potsdam, Institut für Mathematik, Karl-Liebknecht-Str. 24/25, D-14476 Potsdam, Germany (sreich@math.uni-potsdam.de) and University of Reading, Department of Mathematics and Statistics, Whiteknights, PO Box 220, Reading RG6 6AX, UK.

ensemble are in agreement with their importance sampling estimates from a Bayesian inference step. Second-order accurate variants of EnKFs have been considered in [12, 20] before. Here we instead consider second-order corrections to the ETPF. Such corrections require the solution of a continuous-time algebraic Riccati equation [22, 10]. The correction term vanishes as the ensemble size approaches infinity in agreement with the consistency of the ETPF [16].

The paper is organized as follows. The general framework of ensemble transform filters is summarized in Section 2. Section 3 summarizes the ETPF, introduces the second-order correction step, and discusses the numerical solution procedure for the associated continuous-time algebraic Riccati equation. The Sinkhorn approximation to the optimal transport problem of the ETPF is discussed in Section 4 and the overall second-order accurate implementation of the ETPF is summarized in Section 5. Numerical results are provided in Section 6, where the behavior of the new method is demonstrated first for a single Bayesian inference step and then for the highly nonlinear and chaotic Lorenz-63 model [13]. Here we repeat the experiments from [4] with the hybrid ensemble transform particle filter being replaced by a second-order accurate variant based on the Sinkhorn approximation to the underlying optimal transport problem. We finally also demonstrate the behavior of the new filters for parameter estimation of the scene-viewing model *Scene Walk* [7].

## 2 Ensemble-based forecasting-data assimilation systems

Let us assume that observations  $\mathbf{y}^{\text{obs}}(t_k) \in \mathbb{R}^{N_y}$  become available at time instances  $t_k$ ,  $k = 1, \dots, K$ , and are related to the state variables  $\mathbf{z} \in \mathbb{R}^{N_z}$  of an evolution model

$$\mathbf{z}(t_k) = \mathcal{M}(\mathbf{z}(t_{k-1})) \quad (1)$$

via the likelihood function

$$\pi(\mathbf{y}|\mathbf{z}) = \frac{1}{(2\pi)^{N_y/2}|\mathbf{R}|^{1/2}} \exp\left(-\frac{1}{2}(h(\mathbf{z}) - \mathbf{y})^T \mathbf{R}^{-1}(h(\mathbf{z}) - \mathbf{y})\right), \quad (2)$$

where  $\mathbf{R} \in \mathbb{R}^{N_y \times N_y}$  denotes the measurement error covariance matrix.

An ensemble-based forecasting-data assimilation (FOR-DA) systems will produce two sets of ensembles of size  $M$  at any  $t_k$ . First we have the forecast ensemble  $\{\mathbf{z}_i^f\}_{i=1}^M$  which approximates the conditional distribution  $\pi(\mathbf{z}, t_k | \mathbf{y}_{1:k-1}^{\text{obs}})$  and, second, we have the analysis ensemble  $\{\mathbf{z}_i^a\}_{i=1}^M$ , which approximates the conditional distribution  $\pi(\mathbf{z}, t_k | \mathbf{y}_{1:k}^{\text{obs}})$ . Here

$$\mathbf{y}_{1:l}^{\text{obs}} = (\mathbf{y}^{\text{obs}}(t_1), \mathbf{y}^{\text{obs}}(t_2), \dots, \mathbf{y}^{\text{obs}}(t_l)) \in \mathbb{R}^{N_y \times l} \quad (3)$$

denotes the complete set of observations from  $t = t_1$  to  $t = t_l$ . Also note that

$$\mathbf{z}_i^f(t_k) = \mathcal{M}(\mathbf{z}_i^a(t_{k-1})) \quad (4)$$

and that FOR-DA systems primarily differ in the employed data assimilation algorithms.

The data assimilation algorithms considered in this paper are all of the form of a linear ensemble transform filter (LETf) [17]:

$$\mathbf{z}_j^a(t_k) = \sum_{i=1}^M \mathbf{z}_i^f(t_k) d_{ij}(t_k) \quad (5)$$

with the  $M \times M$  transformation matrix  $\mathbf{D}(t_k) = \{d_{ij}(t_k)\}$  defined appropriately. For example, it is well known, that EnKFs can be formulated in the form of (5) [8, 17]. Note that the entries of  $\mathbf{D}$  can be negative. See [17].

The main focus of this paper is, however, on an extension of the ETPF [16, 17] to a second-order accurate PF. The transformation matrix of such a filter depends on the forecast ensemble and the normalized importance weights

$$w_i := \frac{\hat{w}_i(t_k)}{\sum_{j=1}^M \hat{w}_j(t_k)} \quad (6)$$

with  $\hat{w}_i(t_k) = \pi(\mathbf{y}(t_k) | \mathbf{z}_i^f(t_k))$ . The specific form of the transformation matrix  $\mathbf{D}$  will be discussed in Section 3. Since we only rely on importance weights, our filter is also applicable to non-Gaussian likelihood functions. The ETPF can also be applied to spatially extended systems using the idea of localization [3] and has been combined with EnKFs in an hybridization approach [4].

The nonlinear ensemble transform filter (NETF) of [20] provides another example of an LETF, which is based on the importance weights (6). The NETF matches the empirical mean and covariance matrix of a Bayesian inference step and it is therefore called second-order accurate. The details of the NETF are described in Section 3.

While the ETPF convergence to the true posterior distribution in the limit of  $M \rightarrow \infty$  [16], this is not the case for the NETF. However, the ETPF is computationally expensive and underestimates the ensemble spread (covariance matrix) for finite ensemble sizes. Both of these shortcomings will be addressed by the LETFs proposed in Sections 3 and 4.

### 3 Second-order accurate LETFs

We now derive second-order accurate LETFs. Here second-order accuracy refers to reproducing the first and second-order moments exactly according to the importance sampling approach.

**Definition 3.1.** *An LETF (5) is called second-order accurate if the analysis mean satisfies*

$$\bar{\mathbf{z}}^a(t_k) = \frac{1}{M} \sum_{i=1}^M \mathbf{z}_i^a(t_k) = \sum_{i=1}^M w_i(t_k) \mathbf{z}_i^f(t_k) \quad (7)$$

and the analysis covariance matrix

$$\hat{\mathbf{P}}^a(t_k) = \frac{1}{M} \sum_{i=1}^M (\mathbf{z}_i^a(t_k) - \bar{\mathbf{z}}^a(t_k))(\mathbf{z}_i^a(t_k) - \bar{\mathbf{z}}^a(t_k))^T \quad (8)$$

is equal to the covariance matrix defined by the importance weights, i.e.

$$\mathbf{P}^a(t_k) = \sum_{i=1}^M w_i(t_k) (\mathbf{z}_i^f(t_k) - \bar{\mathbf{z}}^a(t_k))(\mathbf{z}_i^f(t_k) - \bar{\mathbf{z}}^a(t_k))^T. \quad (9)$$

Since we only consider the analysis step we drop the explicit time-dependence in the following discussion. We introduce the  $N_z \times M$  matrix of the forecast ensemble

$$\mathbf{Z}^f = (\mathbf{z}_1^f, \mathbf{z}_2^f, \dots, \mathbf{z}_M^f) \in \mathbb{R}^{N_z \times M} \quad (10)$$

and an analog expression

$$\mathbf{Z}^a = (\mathbf{z}_1^a, \mathbf{z}_2^a, \dots, \mathbf{z}_M^a) \in \mathbb{R}^{N_z \times M} \quad (11)$$

for the analysis ensemble. Then an LETF (5) can be represented in the form

$$\mathbf{Z}^a = \mathbf{Z}^f \mathbf{D}. \quad (12)$$

We also introduce the vector  $\mathbf{1} = (1, 1, \dots, 1)^T \in \mathbb{R}^{M \times 1}$  and the vector

$$\mathbf{w} = (w_1, \dots, w_M)^T \in \mathbb{R}^{M \times 1} \quad (13)$$

of normalized importance weights (6) and the diagonal  $M \times M$  matrix  $\mathbf{W} = \text{diag}(\mathbf{w})$ . The importance sampling estimate of the posterior covariance matrix (9) can now be expressed compactly as

$$\mathbf{P}^a = \mathbf{Z}^f (\mathbf{W} - \mathbf{w} \mathbf{w}^T) (\mathbf{Z}^f)^T, \quad (14)$$

while (8) can be written in the form

$$\hat{\mathbf{P}}^a = \frac{1}{M} \mathbf{Z}^f (\mathbf{D} - \mathbf{w} \mathbf{1}^T) (\mathbf{D} - \mathbf{w} \mathbf{1}^T)^T (\mathbf{Z}^f)^T. \quad (15)$$

Since the analysis mean is provided by (7), an LETF is first-order accurate if

$$\frac{1}{M} \mathbf{Z}^a \mathbf{1} = \mathbf{Z}^f \mathbf{w} \quad (16)$$

which is equivalent to

$$\frac{1}{M}\mathbf{D}\mathbf{1} = \mathbf{w}. \quad (17)$$

Note also that any transformation matrix has to satisfy  $\mathbf{D}^T\mathbf{1} = \mathbf{1}$  [17].

Hence, let  $\mathbf{D}$  be an  $M \times M$  transformation matrix with non-negative entries and

$$\sum_{i=1}^M d_{ij} = 1, \quad \sum_{j=1}^M d_{ij} = w_i M. \quad (18)$$

These conditions are, for example, satisfied by the transformation matrix

$$\mathbf{D} = \mathbf{w}\mathbf{1}^T, \quad (19)$$

which leads to the analysis ensemble

$$\mathbf{Z}^a = \bar{\mathbf{z}}^a \mathbf{1}^T \quad (20)$$

However, the implied analysis covariance matrix (15) becomes identical zero, which is clearly undesirable.

The ETPF circumvents this collapse of ensemble spread by requiring that  $\mathbf{D}$  minimizes the cost functional

$$J(\mathbf{D}) = \sum_{i,j=1}^M d_{ij} \|\mathbf{z}_i^f - \mathbf{z}_j^f\|^2 \quad (21)$$

under the constraints  $d_{ij} \geq 0$  and (18) [16]. However the analysis covariance matrix of the ETPF still underestimates the posterior covariance matrix (14). We therefore seek an adjusted transformation

$$\hat{\mathbf{D}} = \mathbf{D} + \mathbf{\Delta} \quad (22)$$

with  $M \times M$  matrix  $\mathbf{\Delta}$  such that  $\mathbf{\Delta}\mathbf{1} = \mathbf{0}$  and  $\mathbf{P}^a = \hat{\mathbf{P}}^a$  with

$$\hat{\mathbf{P}}^a = \frac{1}{M} \mathbf{Z}^f (\hat{\mathbf{D}} - \mathbf{w}\mathbf{1}^T) (\hat{\mathbf{D}} - \mathbf{w}\mathbf{1}^T)^T (\mathbf{Z}^f)^T. \quad (23)$$

The condition

$$\mathbf{0} = \mathbf{P}^a - \hat{\mathbf{P}}^a = \mathbf{Z}^f \left\{ (\mathbf{W} - \mathbf{w}\mathbf{w}^T) - \frac{1}{M} (\hat{\mathbf{D}} - \mathbf{w}\mathbf{1}^T) (\hat{\mathbf{D}} - \mathbf{w}\mathbf{1}^T)^T \right\} (\mathbf{Z}^f)^T, \quad (24)$$

together with (22) lead to the following quadratic equation in the correction  $\mathbf{\Delta}$ :

$$M(\mathbf{W} - \mathbf{w}\mathbf{w}^T) - (\mathbf{D} - \mathbf{w}\mathbf{1}^T)(\mathbf{D} - \mathbf{w}\mathbf{1}^T)^T = (\mathbf{D} - \mathbf{w}\mathbf{1}^T)\mathbf{\Delta}^T + \mathbf{\Delta}(\mathbf{D} - \mathbf{w}\mathbf{1}^T)^T + \mathbf{\Delta}\mathbf{\Delta}^T. \quad (25)$$

The special case (19) leads to

$$\hat{\mathbf{D}} = \mathbf{w}\mathbf{1}^T + \mathbf{\Delta} \quad (26)$$

and a solution of (25) is simply given by

$$\mathbf{\Delta} = \sqrt{M}(\mathbf{W} - \mathbf{w}\mathbf{w}^T)^{1/2}, \quad (27)$$

which recovers the NETF [20, 23]. Note that  $\mathbf{\Delta}\mathbf{Q}$  with  $\mathbf{Q}$  an  $M \times M$  orthogonal matrix also provide a solution to (25) if  $\mathbf{D} = \mathbf{w}\mathbf{1}^T$ .<sup>1</sup> The following proposition states conditions under which the orthogonal matrix  $\mathbf{Q}$  can be defined in an optimal way.

**Proposition 3.2.** *Let  $\mathbf{\Delta}$  be any symmetric  $M \times M$  matrix such that (i)  $\mathbf{\Delta}\mathbf{1} = \mathbf{0}$  and (ii)*

$$\frac{1}{M} \mathbf{\Delta}\mathbf{\Delta} = \mathbf{W} - \mathbf{w}\mathbf{w}^T \quad (28)$$

and let us assume that  $M \leq N_z + 1$ . Define the  $M \times M$  orthogonal matrix

$$\mathbf{Q}_{\text{opt}} := \mathbf{U}_{\text{opt}} \mathbf{V}_{\text{opt}}^T \quad (29)$$

---

<sup>1</sup>The NETF, as proposed in [20], uses randomly chosen orthogonal matrices which satisfy  $\mathbf{Q}\mathbf{1} = \mathbf{1}$  while the NETF of [23] is based on a non-symmetric square root of  $\mathbf{W} - \mathbf{w}\mathbf{w}^T$ .

with the two  $M \times M$  orthogonal matrices  $\mathbf{U}_{\text{opt}}$  and  $\mathbf{V}_{\text{opt}}$  given by the singular value decomposition of the  $M \times M$  matrix

$$\mathbf{S} = \Delta(\widehat{\mathbf{Z}}^f)^T \widehat{\mathbf{Z}}^f, \quad \widehat{\mathbf{Z}}^f := \mathbf{Z}^f - \frac{1}{M} \mathbf{Z}^f \mathbf{1} \mathbf{1}^T, \quad (30)$$

i.e.  $\mathbf{S} = \mathbf{U}_{\text{opt}} \mathbf{\Lambda}_{\text{opt}} \mathbf{V}_{\text{opt}}^T$ . Then the transformation matrix

$$\mathbf{D}_{\text{opt}} = \mathbf{w} \mathbf{1}^T + \Delta \mathbf{Q}_{\text{opt}} \quad (31)$$

results in a second-order accurate LETF, which minimizes

$$\widehat{J}(\mathbf{D}) = \frac{1}{M} \sum_{i=1}^M \|\mathbf{z}_i^a - \mathbf{z}_i^f\|^2 \quad (32)$$

over all second-order accurate transformation matrices  $\mathbf{D}$ .

*Proof.* Since  $\widehat{\mathbf{Z}}^f \mathbf{1} = \mathbf{0}$ , the matrix  $\mathbf{S}$  also satisfies  $\mathbf{S} \mathbf{1} = \mathbf{0}$  in addition to  $\mathbf{S}^T \mathbf{1} = \mathbf{0}$ , which implies that  $\mathbf{Q}_{\text{opt}} \mathbf{1} = \mathbf{1}$  and (31) is second-order accurate. Also note that

$$\left( \Delta(\widehat{\mathbf{Z}}^f)^T \widehat{\mathbf{Z}}^f (\widehat{\mathbf{Z}}^f)^T \widehat{\mathbf{Z}}^f \Delta \right)^{-1/2} \Delta(\widehat{\mathbf{Z}}^f)^T \widehat{\mathbf{Z}}^f = (\mathbf{S} \mathbf{S}^T)^{-1/2} \mathbf{S} \quad (33)$$

$$= (\mathbf{U}_{\text{opt}} \mathbf{\Lambda}_{\text{opt}}^{-1} \mathbf{U}_{\text{opt}}^T) \mathbf{U}_{\text{opt}} \mathbf{\Lambda}_{\text{opt}} \mathbf{V}_{\text{opt}}^T \quad (34)$$

which has been shown in [15] to minimize (32) for given forecast and analysis means and covariance matrices and the optimality of  $\mathbf{Q}_{\text{opt}} = \mathbf{U}_{\text{opt}} \mathbf{V}_{\text{opt}}^T$  follows. See also [17].  $\square$

**Remark 3.3.** If the number of samples,  $M$ , exceeds the dimensions of state space,  $N_z$ , then it is computationally preferable to implement the optimal transformation in the form

$$\mathbf{z}_i^a = \bar{\mathbf{z}}^a + \mathbf{T}(\mathbf{z}_i^f - \bar{\mathbf{z}}^f), \quad (35)$$

where  $\mathbf{T} \in \mathbb{R}^{N_z \times N_z}$  is an appropriately defined symmetric matrix [15, 17]. Alternatively, one could still proceed with (29) but should multiply  $\mathbf{Q}_{\text{opt}}$  by the project matrix  $\mathbf{I} - \mathbf{1} \mathbf{1}^T / M$  from the right in order to keep the resulting transformation matrix  $\mathbf{D}$  mean preserving. This additional operation arises from the fact that the matrix  $\mathbf{S}$  will have multiple zero singular values.

We now return to the general case of a first-order accurate transformation matrix  $\mathbf{D}$ . Then (25) leads to a continuous-time algebraic Riccati equation in the correction  $\Delta$  with the right hand side of the equation being symmetric positive semi-definite. We can now either use the  $\mathbf{D}$  from the ETPF and derive a second-order accurate version of the ETPF or we compute an approximate solution to the optimal transport problem (21) subject to (18) and are still able to turn it into a second-order accurate PF. This aspect will be discussed in more detail in Section 4. We continue here with describing a solution procedure for the continuous-time algebraic Riccati equation.

Upon introducing

$$\mathbf{B} = \mathbf{D} - \mathbf{w} \mathbf{1}^T, \quad \mathbf{A} = M(\mathbf{W} - \mathbf{w} \mathbf{w}^T) - \mathbf{B} \mathbf{B}^T \quad (36)$$

the continuous-time algebraic Riccati equation (25) can be expressed as

$$\mathbf{A} = \mathbf{B} \Delta^T + \Delta \mathbf{B}^T + \Delta \Delta^T. \quad (37)$$

Such an equation can be solved efficiently by applying the Schur vector approach of [10]. The Schur vector approach is based on the extended Hamiltonian matrix

$$\mathbf{H} = \begin{pmatrix} \mathbf{B}^T & \mathbf{I} \\ \mathbf{A} & -\mathbf{B} \end{pmatrix} \quad (38)$$

and its upper triangular Schur decomposition

$$\mathbf{U}^T \mathbf{H} \mathbf{U} = \begin{pmatrix} \mathbf{S}_{11} & \mathbf{S}_{12} \\ \mathbf{0} & \mathbf{S}_{22} \end{pmatrix} \quad (39)$$

with the real part of the spectrum of  $\mathbf{S}_{11}$  being negative and the real parts of the spectrum of  $\mathbf{S}_{22}$  being positive.<sup>2</sup> With the orthogonal matrix  $\mathbf{U}$  partitioned accordingly, the solution of (25) is given by

$$\Delta = \mathbf{U}_{21} \mathbf{U}_{11}^{-1}. \quad (40)$$

We can also seek an optimized  $\Delta$  by computing the singular value decomposition of the matrix  $\Delta(\hat{\mathbf{Z}}^f)^T \hat{\mathbf{Z}}^f$  and the associated orthogonal matrix  $\mathbf{Q}_{\text{opt}} = \mathbf{U}_{\text{opt}} \mathbf{V}_{\text{opt}}^T$  as in (29). We then perform another Schur decomposition of (38) with  $\mathbf{B}$  replaced by  $\mathbf{B} \mathbf{Q}_{\text{opt}}^T$  and finally set

$$\Delta_{\text{opt}} = \mathbf{U}_{21} \mathbf{U}_{11}^{-1} \mathbf{Q}_{\text{opt}} \quad (41)$$

and

$$\hat{\mathbf{D}} = \mathbf{D} + \Delta_{\text{opt}}. \quad (42)$$

## 4 Sinkhorn approximation to the optimal transport problem

The Sinkhorn approximation to the optimal transport problem defined by the cost functional (21) and the constraints (18) is provided by the regularised cost functional

$$J_{\text{SH}}(\mathbf{D}) = \sum_{i,j=1}^M \left\{ d_{ij} \|\mathbf{z}_i^f - \mathbf{z}_j^f\|^2 + \frac{1}{\lambda} d_{ij} \ln d_{ij} \right\} \quad (43)$$

where  $\lambda > 0$  is a regularization parameter. Note that  $\lambda \rightarrow \infty$  leads back to the original cost function (21). The choice  $\lambda \rightarrow 0$ , on the other hand, leads to (19) as the unique minimizer. Hence the parameter  $\lambda$  allows one to naturally bridge between the NETF ( $\lambda = 0$ ) and the second-order corrected ETPF ( $\lambda = \infty$ ). Furthermore, there exists an efficient iterative method for finding the minimizer of (43). First one notes that the minimizer is of the form

$$\mathbf{D} = \text{diag}(\mathbf{u}) \mathbf{K} \text{diag}(\mathbf{v}), \quad (44)$$

where  $\mathbf{u} \in \mathbb{R}^{M \times 1}$  and  $\mathbf{v} \in \mathbb{R}^{M \times 1}$  are two non-negative vectors ensuring that  $\mathbf{D}$  satisfies the constraints (18) and  $\mathbf{K}$  has entries

$$k_{ij} = e^{-\lambda \|\mathbf{z}_i^f - \mathbf{z}_j^f\|^2}. \quad (45)$$

The unknown vectors  $\mathbf{u}$  and  $\mathbf{v}$  can be computed by Sinkhorn's fixed point iteration

$$\{Mw_i/(\mathbf{K}\mathbf{v})_i\} \rightarrow \mathbf{u}, \quad \{1/(\mathbf{K}\mathbf{u})_i\} \rightarrow \mathbf{v}. \quad (46)$$

See [5] for an efficient implementation and additional details.

Let us denote the iterates of  $\mathbf{u}$  and  $\mathbf{v}$  by  $\mathbf{u}^l$  and  $\mathbf{v}^l$ , respectively, where we always update  $\mathbf{u}$  first according to the formula to the left in (46). Then the associated

$$\mathbf{D}^l = \text{diag}(\mathbf{u}^l) \mathbf{K} \text{diag}(\mathbf{v}^l) \quad (47)$$

satisfies

$$(\mathbf{D}^l)^T \mathbf{1} = \mathbf{1} \quad (48)$$

and the weights

$$\mathbf{w}^l = \frac{1}{M} \mathbf{D}^l \mathbf{1} \quad (49)$$

converge to  $\mathbf{w}$  as  $l \rightarrow \infty$ . If we stop the iteration at an index  $l_*$ , then we define the associated transformation matrix by

$$\mathbf{D} = \mathbf{D}^{l_*} - (\mathbf{w}^{l_*} + \mathbf{w}) \mathbf{1}^T. \quad (50)$$

This is followed by the computation of the associated correction matrix  $\Delta_{\text{opt}}$  in order to define a second-order accurate LETF. The index  $l_*$  can be determined by the condition

$$\|\mathbf{w}^{l_*} - \mathbf{w}\| \leq \varepsilon \quad (51)$$

for sufficiently small  $\varepsilon > 0$ , e.g.  $\varepsilon = 10^{-8}$ .

---

<sup>2</sup>If the matrix pair  $(\mathbf{B}, \mathbf{I})$  is stabilizable and the matrix pair  $(\mathbf{A}^{1/2}, \mathbf{B})$  is detectable, then the Hamiltonian matrix  $\mathbf{H}$  possesses real eigenvalues only [22] and a decomposition of the form (39) exists [10].

## 5 Algorithmic summary

We summarise the key steps of the second-order accurate ETPF implementation. We assume that a given set of forecast ensemble members  $\mathbf{Z}^f$  and a vector of importance weights  $\mathbf{w}$  are given. Then the following steps are performed:

- (i) Select a regularization parameter  $\lambda > 0$  for the Sinkhorn approximation to the optimal transport algorithm. Compute the matrix  $\mathbf{K}$  according to (45). Normalize the entries of  $\mathbf{K}$  such that all entries satisfy  $-\lambda^{-1} \ln k_{ij} \leq 1$ . Recursively compute vectors  $\mathbf{u}^l$  and  $\mathbf{v}^l$  according to the update formula (46). Start with  $\mathbf{v}^0 = \mathbf{1}$ . Iterate till the transformation matrix (47) and its associated weight vector (49) satisfy (51). Note that (47) should satisfy  $\mathbf{1}^T \mathbf{D}^l = \mathbf{1}^T$  in each iteration. We used  $\varepsilon = 10^{-8}$  in our experiments. Set  $\mathbf{D} = \mathbf{D}^{l*}$ .
- (ii) Solve the Riccati equation for the correction  $\Delta$  using the upper triangular Schur decomposition of (38) with  $\mathbf{A}$  and  $\mathbf{B}$  as defined in (36). The correction is then given by (40).<sup>3</sup>
- (iii) Compute the optimized update  $\Delta_{\text{opt}}$ . This requires the singular value decomposition  $\mathbf{U}_{\text{opt}} \mathbf{\Lambda}_{\text{opt}} \mathbf{V}_{\text{opt}}^T$  of  $\Delta(\hat{\mathbf{Z}}^f)^T \hat{\mathbf{Z}}^f$ , which yields  $\mathbf{Q}_{\text{opt}} = \mathbf{U}_{\text{opt}} \mathbf{V}_{\text{opt}}^T$ . See (30) for the definition of the matrix  $\hat{\mathbf{Z}}^f$  of forecast ensemble perturbations. Next solve the Riccati equation with  $\mathbf{B}$  replaced by  $\mathbf{B} \mathbf{Q}_{\text{opt}}^T$ . Denote the solution again by  $\Delta$ . Finally, set  $\Delta_{\text{opt}} = \Delta \mathbf{Q}_{\text{opt}}$  and define the corrected transformation matrix,  $\hat{\mathbf{D}}$ , by (42).
- (iv) The analysis ensemble is given by

$$\mathbf{Z}^a = \mathbf{Z}^f \hat{\mathbf{D}}. \quad (52)$$

The second-order accurate ETPF requires the computation of singular value and Schur decompositions of  $M \times M$  matrices. Those can be performed in  $\mathcal{O}(M^3)$  operations. The Sinkhorn approximation requires  $\mathcal{O}(M^2)$  operations [5]. Hence the computational complexity of the second-order accurate ETPF is of the same order in  $M$  as for EnKFs.

We mention that the proposed second-order accurate ETPF can be used instead of the standard ETPF in a hybrid filter, as described in [4], and, when applied to spatially extended system, can also be used with localization. See [17, 3] for details.

## 6 Numerical examples

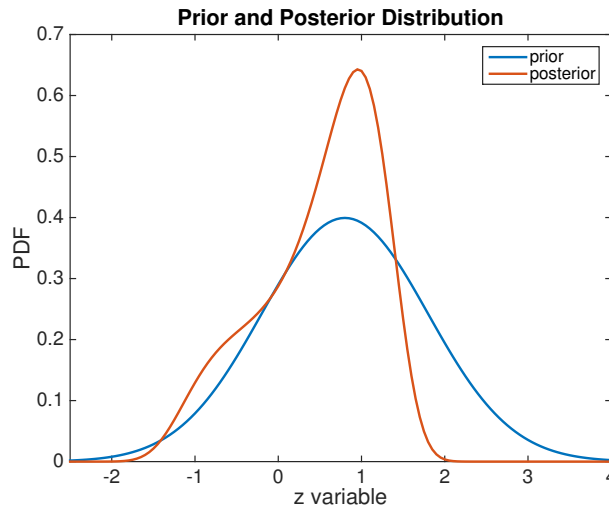


Figure 1: Prior and posterior distribution for the single Bayesian inference step.

<sup>3</sup>We use the MATLAB routines `schur` and `ordschur` to compute the Schur decomposition (39). If the associated (40) fails to provide a solution to the algebraic Riccati equation (25), then we use the correction  $\Delta = \mathbf{A}^{1/2}$  instead.

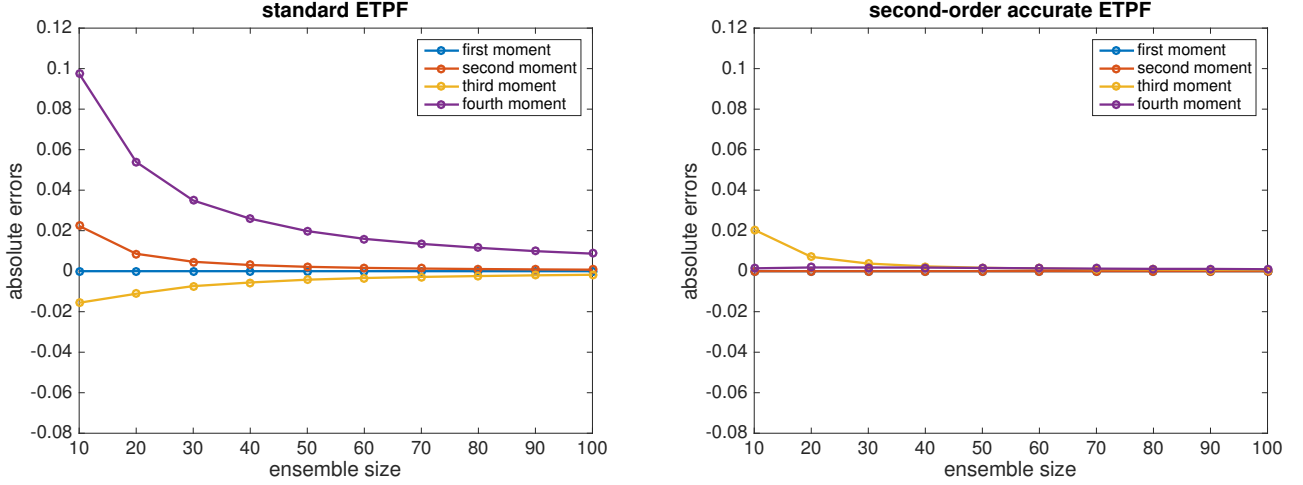


Figure 2: Absolute errors in the first four moments of the posterior distribution as obtained from the standard ETPF (left panel) and the second-order corrected ETPF (right panel).

We now demonstrate the numerical behavior of the proposed second-order accurate ETPF as summarized in Section 5. We first analyze a single Bayesian inference step. The second experiment is based on the Lorenz-63 model and its data assimilation setting of [4]. We finally apply the second-order accurate filters to parameter estimation of the scene-viewing model *SceneWalk* [7].

## 6.1 A univariate Bayesian inference problem

We consider a univariate Bayesian inference problem with Gaussian prior with mean  $\bar{z} = 0.8$  and variance equal to one, likelihood function

$$\pi(y|z) \propto \exp\left(-\frac{1}{2}(z^2 - y)^2\right)$$

and observed value  $y_{\text{obs}} = 1$ . The non-Gaussian posterior distribution can be found in Figure 1.

We implement the second-order accurate ETPF for ensemble sizes  $M \in \{10, 20, 30, \dots, 90, 100\}$  and compare it to the standard ETPF implementation. We compute the errors in the resulting first four moments and repeat each experiment ten thousand times. The resulting averaged errors can be found in Figure 2.

We also implemented the second-order ETPF using the Sinkhorn approximation, as described in Section 5), with regularization parameter  $\lambda = 10$  and  $\lambda = 100$ . The results can be found in Figure 3. Not shown are the results for  $\lambda = 0$  (which corresponds to the NETF), which yield an error of about 0.11 in the third moment and an error of about -0.2 in the fourth moment for all ensemble sizes.

We conclude that the second-order accurate ETPF provides a significant improvement over the standard ETPF. It is also found that the regularization parameter,  $\lambda$ , needs to be chosen sufficiently large in order to provide a satisfactory performance of the Sinkhorn approximation.

## 6.2 Lorenz-63

We use the chaotic Lorenz-63 system [13] with the standard parameter setting  $\sigma = 10$ ,  $\rho = 28$ , and  $\beta = 8/3$ , and observe the first component of the three dimensional system in observation intervals of  $\Delta t_{\text{obs}} = 0.12$  with observation error variance  $R = 8$ . A total of  $K = 100,000$  assimilation steps are performed. Since the model dynamics is deterministic, particle rejuvenation

$$\mathbf{z}_j^a \rightarrow \mathbf{z}_j^a + \sum_{i=1}^M (\mathbf{z}_i^f - \bar{\mathbf{z}}^f) \frac{\beta \xi_{ij}}{\sqrt{M-1}} \quad (53)$$

is applied with  $\beta = 0.2$  and  $\xi_{ij}$  independent and identically distributed Gaussian random variables with mean zero and variance one. Simulations with  $\beta = 0.15$  and  $\beta = 0.25$  gave similar results to those reported here.



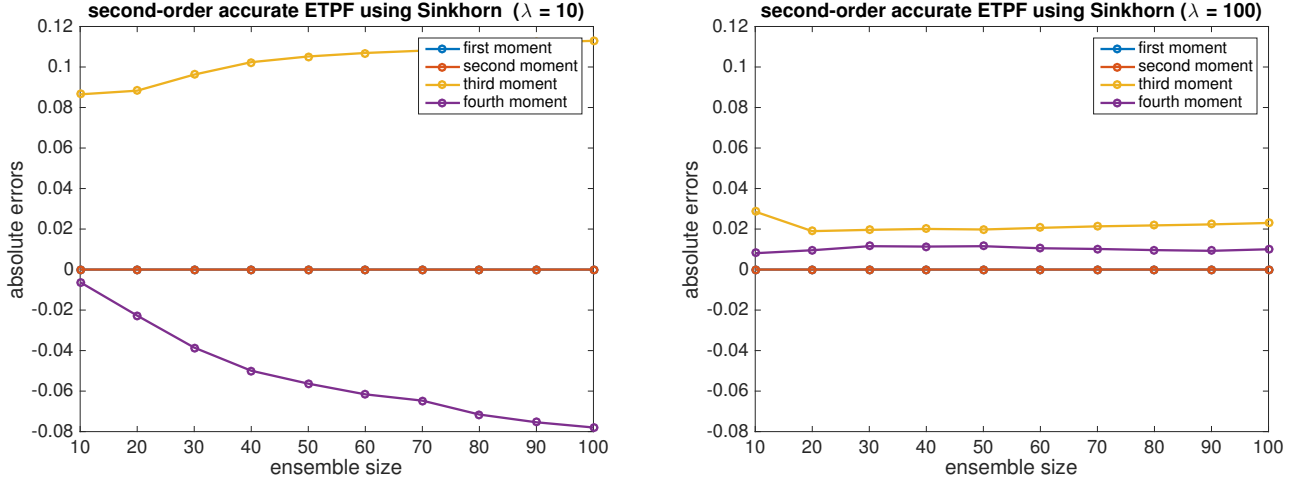


Figure 3: Absolute errors in the first four moments of the posterior distribution as obtained from a second-order accurate ETPF using the Sinkhorn approximation with  $\lambda = 10$  (left panel) and  $\lambda = 100$  (right panel).

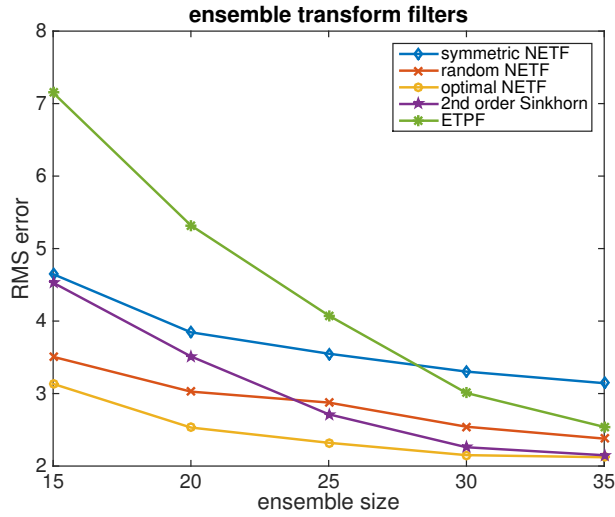


Figure 4: RMSEs for various second-order accurate LETFs compared to the ensemble transform particle filter (ETPF) as a function of the sample size,  $M$ .

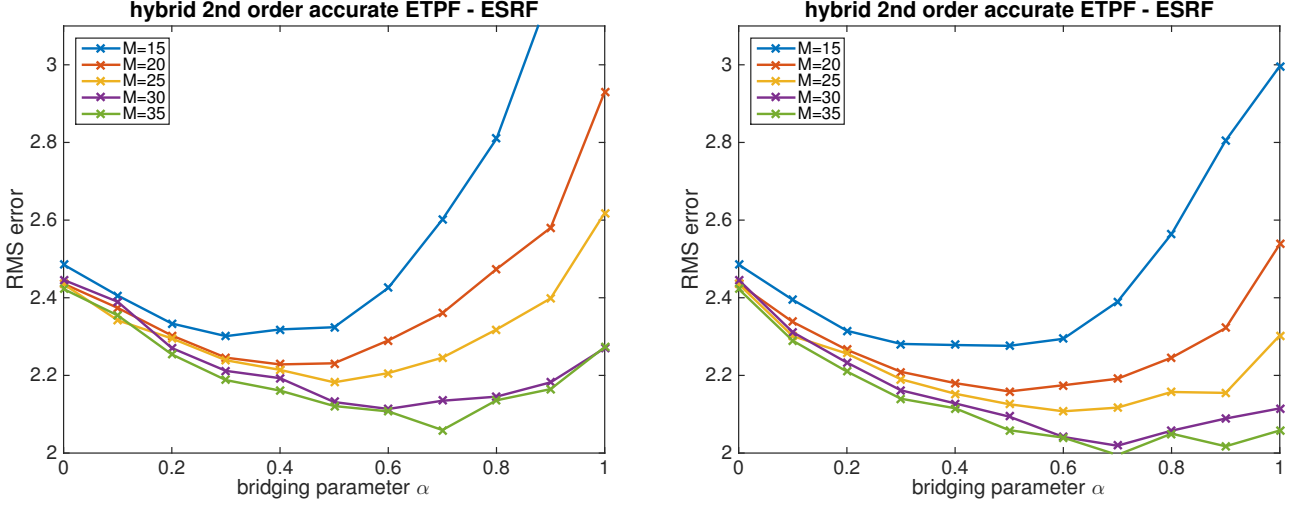


Figure 5: Hybrid filter with second-order accurate ETPF and regularization parameter  $\lambda = 10$  (left panel) and  $\lambda = 40$  (right panel) in the Sinkhorn approximation. Time-averaged RMSEs are displayed as a function of the bridging parameter  $\alpha$ . Please note that  $\alpha = 0$  corresponds to the standard ESRF, while  $\alpha = 1$  corresponds to a purely second-order ETPF.

This data assimilation setting has already been used in [4] since it leads to non-Gaussian forecast and analysis distributions and a particle filter is able to outperform EnKFs in the limit of large ensemble sizes. Here we are, however, interested in the performance of second-order accurate filters for small ensemble sizes in the range  $M \in \{15, 20, \dots, 35\}$ . See Figure 4 for the resulting time-averaged RMSEs. It can be clearly seen that the NETF with optimally chosen rotation matrix leads to the smallest RMSEs. The second-order accurate Sinkhorn filter uses  $\lambda = 40$  and performs well for the larger ensemble sizes. It can also be seen that the standard ETPF is not competitive at the smaller ensemble sizes.

We now test the second-order accurate transform filters within the hybrid filter framework proposed in [4]. More specifically, the hybrid filter of [4] with a second-order accurate transform filter applied first is implemented for ensemble sizes varying between  $M = 15$  and  $M = 35$ . The bridging parameter,  $\alpha$ , of the hybrid filter approach is chosen such that  $\alpha = 0$  corresponds to a standard ensemble square root filter (ESRF) [8] while  $\alpha = 1$  leads to a purely second-order accurate ETPF, as summarized in Section 5. We perform experiments for fixed bridging parameter  $\alpha \in \{0, 0.1, 0.2, \dots, 0.9, 1.0\}$  and regularization parameter  $\lambda \in \{10, 40\}$  in the Sinkhorn approximation to the optimal transport problem of the second-order accurate ETPF.

The time-averaged RMSEs for fixed bridging parameter  $\alpha \in \{0, 0.1, \dots, 0.9, 1.0\}$ , can be found in Figure 5 for  $\lambda = 10$  and  $\lambda = 40$ . While  $\lambda = 10$  leads to time-averages RMSEs which are slightly worse than those from the hybrid filter with a standard ETPF implementation (compare results in [4]), a regularization parameter value of  $\lambda = 40$  leads to improvements especially for larger values of the bridging parameter,  $\alpha$ . Overall we find the behavior of the filter less sensitive to the choice of the regularization parameter,  $\lambda$ , than in the previous univariate example.

We finally implemented the hybrid filter of [4] with the ETPF being replaced by the second-order accurate NETF with the rotation matrix,  $\mathbf{Q}$ , defined as in (29). We denote this hybrid filter by NETF-ESRF. The resulting RMSEs can be found in Figure 6. The optimal RMSEs for the hybrid NETF-ESRF for given ensemble size,  $M$ , are quite similar to those displayed in Figure 5 and to those of the hybrid ETPF-ESRF method of [4]. However, it is found that the optimal values of the bridging parameter,  $\alpha$ , are shifted towards larger values for all the second-order accurate methods. We also display the RMSEs for implementations of the NETF with randomly chosen orthogonal matrices,  $\mathbf{Q}$ , as suggested by [20] in Figure 6. It can be seen that randomly chosen orthogonal matrices lead to substantially increased RMSEs.

### 6.3 Estimating parameters for a dynamic scene viewing model

The scene-viewing model *SceneWalk*, as recently proposed by [7], dynamically evolves a two-dimensional array of probabilities,  $\pi_{ij}(t)$ , for the next fixation target. The model consists of two sets of ordinary differential

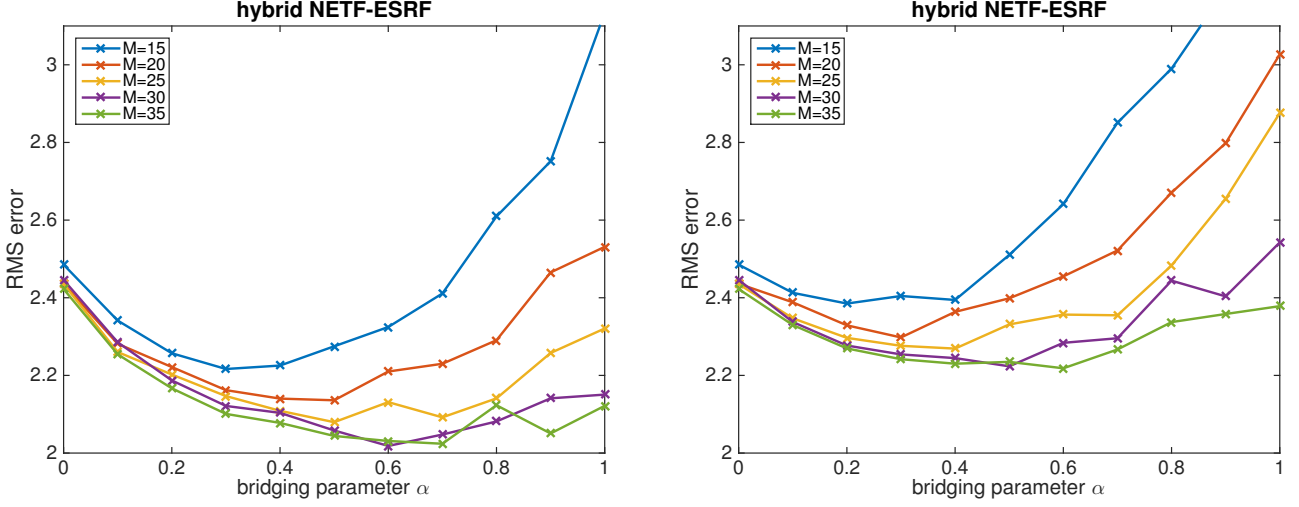


Figure 6: Hybrid NETF-ESRF with the the orthogonal matrix  $\mathbf{Q}$  as defined in (29) (left panel) and randomly chosen orthogonal matrix as suggested in [20] (right panel). Time-averaged RMSEs are displayed as a function of the bridging parameter  $\alpha$ .

equations

$$\frac{dA_{ij}(t)}{dt} = -\omega_A A_{ij}(t) + \omega_A \frac{S_{ij} \cdot G_A(x_i, y_j; x_f, y_f)}{\sum_{kl} S_{kl} \cdot G_A(x_k, y_l; x_f, y_f)} \quad (54)$$

$$\frac{dF_{ij}(t)}{dt} = -\omega_F F_{ij}(t) + \omega_F \frac{G_F(x_i, y_j; x_f, y_f)}{\sum_{kl} G_F(x_k, y_l; x_f, y_f)} \quad (55)$$

for the spatial attention and fixation, respectively, together with a set of transformation rules

$$u_{ij}(t) = \frac{[A_{ij}(t)]^\lambda}{\sum_{kl} [A_{kl}(t)]^\lambda} - c_{inhib} \frac{[F_{ij}(t)]^\gamma}{\sum_{kl} [F_{kl}(t)]^\gamma}, \quad (56)$$

$$u^*(u) = \begin{cases} u & u > \eta \\ \eta e^{\frac{u-\eta}{\eta}} & u \leq \eta \end{cases}, \quad (57)$$

which finally produce the desired array of fixation probabilities

$$\pi_{ij}(t) = (1 - \zeta) \frac{u_{ij}^*(t)}{\sum_{kl} u_{kl}^*(t)} + \zeta \frac{1}{\sum_{kl} 1}. \quad (58)$$

The functions  $G_{A/F}$  in (54)-(55) are Gaussians given by

$$G_{A/F}(x, y; x_f, y_f) = \frac{1}{2\pi\sigma_{A/F}^2} \exp\left(-\frac{(x - x_f)^2 + (y - y_f)^2}{2\sigma_{A/F}^2}\right) \quad (59)$$

and  $\{S_{ij}\}$  is a static saliency map. See [7, 18] for a detailed description of the model. The *SceneWalk* model contains 9 parameters, which have been estimated in [18] using maximum likelihood estimates. Here we estimate  $\sigma_F$  in (59) and  $\omega_F$  in (55) with the remaining seven parameter values taken from [18]. We start from a uniform prior over the interval  $[1, 5]$  for the first variable and a uniform prior over the interval  $[8, 16]$  for the second variable, respectively.

The importance weights resulting from a given pool of scan paths and  $M = 200$  samples from the prior distribution can be found in Figure 7.

We implement the NETF method with  $\mathbf{Q} = \mathbf{I}$  (symmetric NETF), the NETF with the optimal  $\mathbf{Q}$  (optimal NETF), the ETPF, and the second-order accurate ETPF. The distribution of transformed versus prior sample values for each of the two parameters separately can be found in Figure 8. While the optimal NETF leads to a

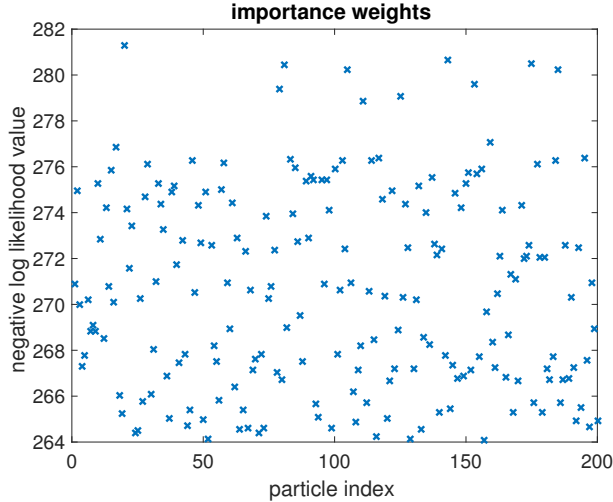


Figure 7: Importance weights for  $M = 200$  samples in two-dimensional parameter space.

nearly linear relation between the prior and transformed samples, the symmetric NETF leads to a rather non-regular structure. At the same time we find that the second-order accurate ETPF leads to large fluctuations in the transformed samples with some samples leaving the prior range. Since this behavior is violating Bayes' law, it must be seen as a undesirable effect of enforcing strict second-order accuracy. The associated two-dimensional scatter plots of the prior and transformed samples can be found in Figure 9. These plots show even more clearly that second-order accurate methods can lead to transformed samples, which violate Bayes' law. Nevertheless, all methods consider qualitatively capture the posterior distribution.

## 7 Conclusions

We have proposed and tested second-order variants of the ETPF. These modifications are computationally attractive since it allows one to replace the computationally expensive solution of an optimal transport problem by its Sinkhorn approximation. Furthermore, if the regularization parameter,  $\lambda$ , in the Sinkhorn approximation is set to zero, then we recover the NETF [20] with an optimally chosen orthogonal matrix  $\mathbf{Q}_{\text{opt}}$  in (29), while  $\lambda \rightarrow \infty$  leads formally back to the optimal transport implementation of the ETPF. As a byproduct, we also found that the NETF with an optimally chosen orthogonal matrix,  $\mathbf{Q}$ , leads to smaller RMSEs compared to a random choice, as suggested in [20].

The second-order accurate ETPF can be put into the hybrid ensemble transform particle framework of [4] and can be combined with localization as necessary for spatially extended evolution equation [8, 17, 3]. Overall, the methodology proposed in this paper together with the hybrid approach of [4] provides a powerful framework for performing sequential data assimilation. We finally mention that all methods considered in this paper can be combined with alternative proposal densities, which lead to more balanced importance weights (6) [21].

It should be noted though, that second-order accuracy comes at a price, i.e., the entries of the transformation matrix  $\hat{\mathbf{D}}$  are not necessarily non-negative, as it is the case for the ETPF transformation matrix  $\mathbf{D}$ . Hence the analysis ensemble is not necessarily contained in the convex hull spanned by the forecast ensemble. This can cause non-physical states if, for example, the states should only take values in a bounded interval or semi-interval, as has been demonstrated for the *SceneWalk* model.

## Acknowledgments

We like to thank Hans-Rudolf Künsch and Sylvain Robert for discussions on second-order corrections to linear ensemble transform filters. We also thank Ralf Engbert and Heiko Schütt for providing the data set used in Section 6.3.

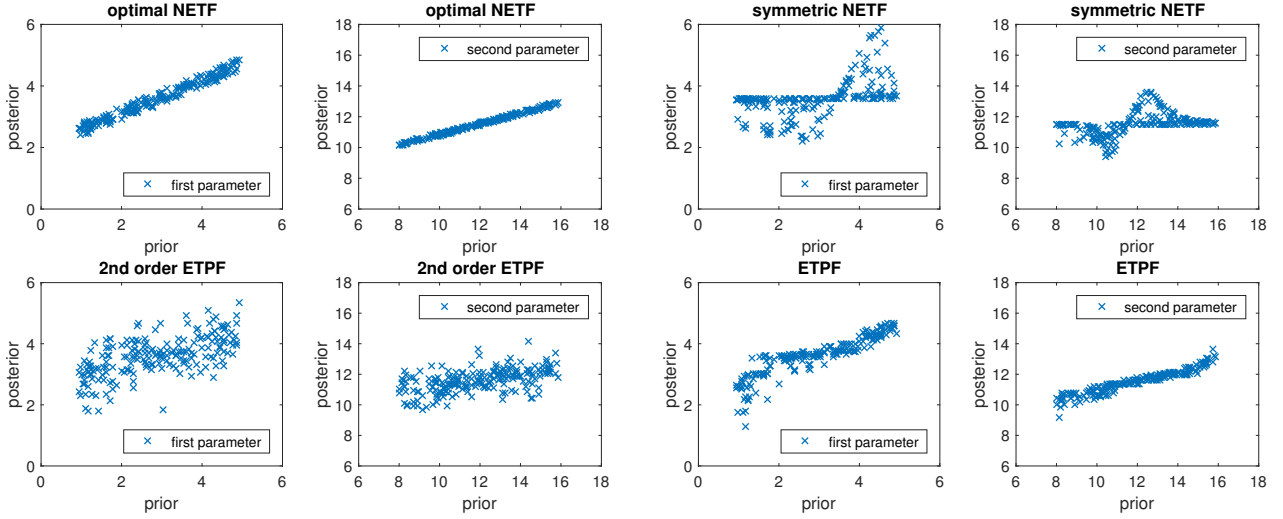


Figure 8: Prior vs posterior samples: optimal NETF (left panel, top row), symmetric NETF (right panel, top row). The two panels also show the ETPF (right panel, bottom row) and the 2nd order corrected ETPF (left panel, bottom row) for comparison. Both the optimal NETF and the ETPF lead to relatively concentrated sample sets, following nearly linear relationships.

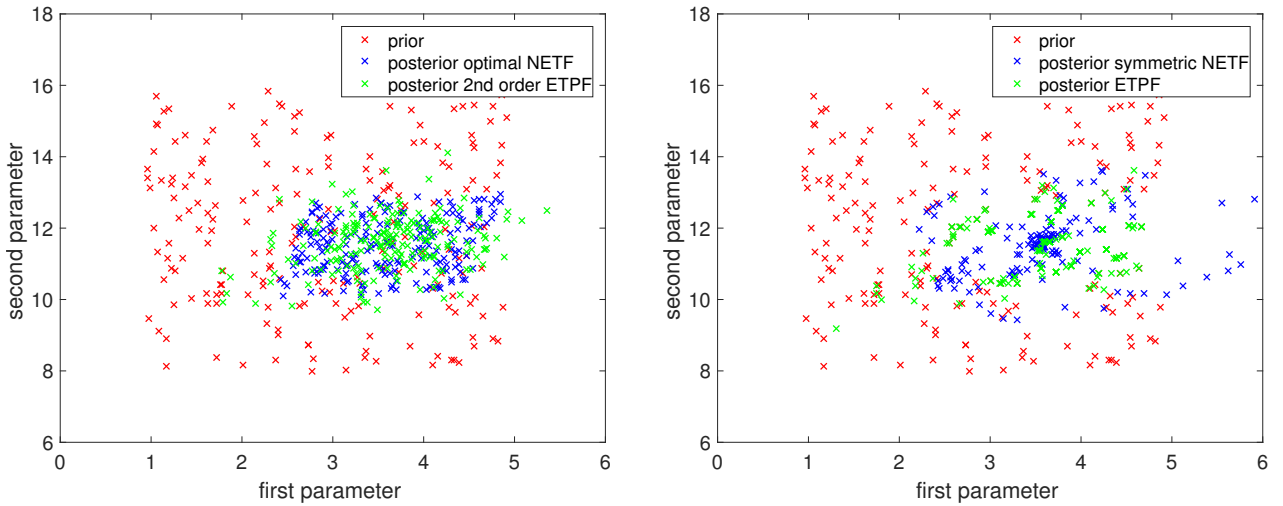


Figure 9: Prior vs posterior samples: optimal NETF (left panel), symmetric NETF (right panel). Both panels show the ETPF and the 2nd-order corrected ETPF, respectively, for comparison. It can be clearly seen that the symmetric NETF and the 2nd order corrected ETPF lead to posterior samples which are outside the range of the prior samples.

## References

- [1] J. ANDERSON, *A non-Gaussian ensemble filter update for data assimilation*, Monthly Weather Review, 138 (2010), pp. 4186–4198.
- [2] T. BENGTTSSON, P. BICKEL, AND B. LI, *Curse of dimensionality revisited: Collapse of the particle filter in very large scale systems*, in IMS Lecture Notes - Monograph Series in Probability and Statistics: Essays in Honor of David F. Freedman, vol. 2, Institute of Mathematical Sciences, 2008, pp. 316–334.
- [3] Y. CHEN AND S. REICH, *Assimilating data into scientific models: An optimal coupling perspective*, in Frontiers in Applied Dynamical Systems: Reviews and Tutorials, vol. 2, Springer-Verlag, New York, 2015, pp. 75–118.
- [4] N. CHUSTAGULPROM, S. REICH, AND M. REINHARDT, *A hybrid ensemble transform filter for nonlinear and spatially extended dynamical systems*, SIAM/ASA J. Uncertainty Quantification, 4 (2016), pp. 592–608.
- [5] M. CUTURI, *Sinkhorn distances: Lightspeed computation of optimal transport*, in NIPS 2013, 2013.
- [6] A. DOUCET, N. DE FREITAS, AND N. G. (EDS.), *Sequential Monte Carlo methods in practice*, Springer-Verlag, Berlin Heidelberg New York, 2001.
- [7] R. ENGBERT, H. A. TRUKENBROD, S. BARTHELMÉ, AND F. A. WICHMANN, *Spatial statistics and attentional dynamics in scene viewing*, Journal of Vision, 15 (2015).
- [8] G. EVENSEN, *Data assimilation. The ensemble Kalman filter*, Springer-Verlag, New York, 2006.
- [9] M. FREI AND H. KÜNSCH, *Bridging the ensemble Kalman and particle filters*, Biometrika, 100 (2013), pp. 781–800.
- [10] A. LAUB, *A Schur method for solving algebraic Riccati equations*, IEEE Trans. Automatic Control, 24 (1979), pp. 913–921.
- [11] K. LAW, A. STUART, AND K. ZYGALAKIS, *Data Assimilation: A Mathematical Introduction*, Springer-Verlag, New York, 2015.
- [12] J. LEI AND P. BICKEL, *A moment matching ensemble filter for nonlinear and non-Gaussian data assimilation*, Mon. Weath. Rev., 139 (2011), pp. 3964–3973.
- [13] E. LORENZ, *Deterministic non-periodic flows*, J. Atmos. Sci., 20 (1963), pp. 130–141.
- [14] S. METREF, E. COSME, C. SNYDER, AND P. BRASSEUR, *A non-Gaussian analysis scheme using rank histograms for ensemble data assimilation*, Nonlinear Processes in Geophysics, 21 (2013), pp. 869–885.
- [15] I. OLKIN AND F. PUKELSHEIM, *The distance between two random vectors with given dispersion matrices*, Linear Algebra and its Applications, 48 (1982), pp. 257–263.
- [16] S. REICH, *A nonparametric ensemble transform method for Bayesian inference*, SIAM J. Sci. Comput., 35 (2013), pp. A2013–A2024.
- [17] S. REICH AND C. COTTER, *Probabilistic Forecasting and Bayesian Data Assimilation*, Cambridge University Press, Cambridge, 2015.
- [18] H. SCHÜTT, L. ROTHKEGEL, H. TRUKENBROD, S. REICH, F. WICHMANN, AND R. ENGBERT, *Likelihood-based parameter estimation and comparison of dynamical cognitive models*, Tech. Rep. ArXiv:1606.07309, University of Potsdam, 2016.
- [19] A. STORDAL, H. KARLSEN, G. NÆVDAL, H. SKAUG, AND B. VALLÉS, *Bridging the ensemble Kalman filter and particle filters: the adaptive Gaussian mixture filter*, Comput. Geosci., 15 (2011), pp. 293–305.
- [20] J. TÖDTER AND B. AHRENS, *A second-order exact ensemble square root filter for nonlinear data assimilation*, Mon. Wea. Rev., 143 (2015), pp. 1347–1367.
- [21] P. VAN LEEUWEN, *Nonlinear data assimilation for high-dimensional systems*, in Frontiers in Applied Dynamical Systems: Reviews and Tutorials, vol. 2, Springer-Verlag, New York, 2015, pp. 1–73.

- [22] W. WONHAM, *On a matrix Riccati equation of stochastic control*, SIAM J. Contr., 6 (1968), pp. 681–697.
- [23] X. XIONG, I. NAVON, AND B. UZUNGOGLU, *A note on the particle filter with posterior Gaussian resampling*, Tellus, 85A (2006), pp. 456–460.